Ohmic contacts fabricated on moderately doped p-type GaAs by sputtering deposition and a laser-firing process

Alfredo Boronat,[a] Santiago Silvestre, and Albert Orpella
MNT—Electronic Engineering Department, Universitat Politècnica de Catalunya, C/ Jordi Girona 1-3, Campus Nord UPC, 08034 Barcelona, Spain

(Received 1 February 2013; accepted 27 August 2013; published 12 September 2013)

A novel approach is used to achieve ohmic contacts on moderately doped p-type GaAs substrates. A laser-firing process is used instead of the conventional annealing step. The morphology of the crater created by the laser-firing process and the electrical response of the metal–semiconductor contact are characterized. © *2013 American Vacuum Society*. [http://dx.doi.org/10.1116/1.4820912]

I. INTRODUCTION

When the potential voltage drop across a metal–semiconductor contact is linearly related to the current, the contact is said to be ohmic, and the contact resistance R_C is the slope of the voltage–current characteristic. The contact voltage drop depends on the specific contact resistivity (ρ_{cef}), the dimensions of the contact area, and the level of electrical current. Two main approaches are used to achieve low ρ_{cef} values on low doped III–V semiconductors:[1,2] (1) creation of a heavily doped layer under the contact area in the semiconductor, and (2) formation of a lower bandgap semiconductor region at the contact interface.

The low barrier heights ($Ø_B \sim 0.5$ eV) of p-type materials and the potential to achieve sufficiently high doping levels allow the formation of ohmic contacts on p-type GaAs. Au-based alloys are the materials most commonly used for both n- and p-type GaAs,[3] with Au/Zn/Au,[4,5] AuBe,[6] and Ti/Pt/Au (Ref. 6) contacts being the most common on p-type GaAs. In most cases, high temperature thermal steps are necessary. However, low temperature processes are required in the fabrication of some electronic devices, including: solar cells, where the use of low temperature processes helps to prevent device degradation;[7,8] new structures related to the Intermediate Band concept, where low temperature is essential to achieve sufficient Ti concentrations;[9] or in applications based on the integration of GaAs films on Si substrates, where thermal stress is an important issue.[10]

In this work, alloyed contacts were fabricated on III–V substrates using a technique in which only a localized region is heated to avoid thermal stresses on the whole structure. Ohmic contacts were fabricated on moderately doped p-type GaAs substrate wafers by sputtering deposition of Au/Zn/Au structures followed by the use of a laser-firing process whereby a pulsed laser beam drives the Zn into the GaAs but also forms a small crater-like structure. Laser fired contacts (LFC) have been successfully applied in other studies to form ohmic contacts.[11–13]

This work is divided in two stages. In the first stage, we investigated how Zn sputtering power conditions influence the electrical characteristics of metal-semiconductor contacts. This stage concluded by using a rapid thermal annealing (RTA) step extracting the substrate resistivity. In the second stage, we analyzed different laser-firing parameters to determine optimal values, taking into account the electrical characteristics of the metal–semiconductor contact and the morphology of the crater created.

II. EXPERIMENTAL METHODS

For substrates, we used commercial (LEC) p-type GaAs single sided polished wafers with 625 μm thickness and Zn doped concentration of $\sim 10^{17}$ cm^{-3}. All metal layers were deposited using an RF Sputtering System ESM100 Edwards & RFS5 Generator-300 W. Zn targets were presputtered for 45 min to clean them prior to each Zn layers deposition. All films were deposited under a constant 10 sccm flux of pure Ar. The total working pressure was kept at 0.2 Pa for Zn layer and at 0.5 Pa for Au layers. The base vacuum of the sputtering chamber before each deposition was less than 9×10^{-4} Pa for all processes. A thermocouple was placed next to the sample exposed to direct impact of sputtered atoms in order to monitor the temperature during the sputtering process.

In this work, the ohmic contacts were fabricated using a multilayer structure of Au/Zn/Au (20 nm/50 nm/250 nm) layer thicknesses were selected based on previous literature.[4,5] The first Au (20 nm) layer is designed to provide good adhesion of the Zn layer and its relative thinness should permit easy penetration of Zn into the GaAs bulk during the alloy process. The Zn (50 nm) layer is the doping source to create the tunneling ohmic contact. The last Au (250 nm) layer prevents vaporization of Zn during the thermal step process.

The substrate was cut into 2 cm $\times$ 2 cm pieces to allow multiple experiments. After cutting, the samples were cleaned in an ultrasonic acetone bath followed by an ultrasonic isopropanol bath to remove any dust deposited during the cutting process.

Figure 1 shows the vertical structure used to evaluate the electrical behavior of the metal–semiconductor contact. First, the unpolished side was covered with the multilayer structure to create a large back contact. Then, round contacts were deposited on the polished side of the substrate. The round contacts were defined by using a shadow mask in order to avoid the need for a lithography step, which typically requires temperatures above 100 °C that could alter the interface either by resin waste or developer reactivity.

[a]Electronic mail: alfredo.boro@gmail.com

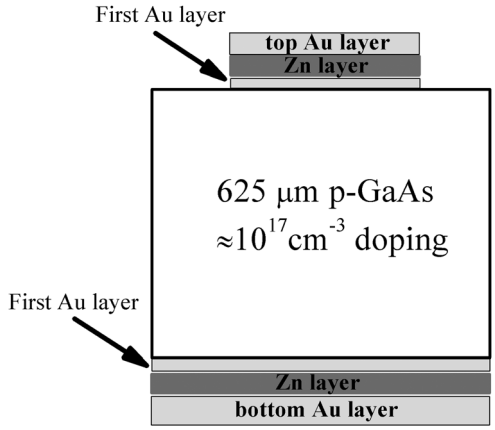

FIG. 1. Schematic cross sections of samples.

The laser system used to carry out this work was a Q-switched Nd:YAG laser (StarMark SMP 100II Rofin-Baassel; Stanberg, Germany), operating at a wavelength of 1064 nm in TEM_{00} mode with a 100 ns pulse duration. The laser power can be adjusted from 0.8 to 6.4 W by varying the pump lamp current (software control parameter). The laser power was measured using a power thermal sensor [OPHIR 30 (150)A-BB-18].

III. RESULTS AND DISCUSSION

A. Effect of the RF sputtering power deposition of the Zn layer

The first stage of this study is focused on selecting favorable RF sputtering conditions, for the different layers especially power and deposition times. A maximum substrate temperature of 50 °C was selected to ensure a low temperature process. It is widely reported that RF power has a direct influence on the energy of atoms sputtered from the target impinging on the substrate.[14] This energy and the deposition time affect the temperature reached by the substrate. The deposition conditions of Au layers for substrate temperatures below 50 °C are detailed in Table I.

The possibility of a Zn diffusion by increasing the RF sputtering power was explored to assess whether increasing RF sputtering power can lead to ohmic contact formation. Powers of 25, 50, and 75 W were used. The low power (25 W) is the minimum power that sputters atoms from the Zn target in our equipment, and the high power (75 W) was established to avoid problems with the reflected sputtering power. The thickness of the Zn layer was fixed at 50 nm, based on previous studies.[4,5] Sputtering conditions for each sample are summarized in Table II.

TABLE I. Sputtering conditions for deposition of Au layers.

Layer	Power (W)	Thickness (nm)	Deposition time (min)	Substrate temperature (°C)
First Au layer	15	20	10	38
Top Au layer	25	250	40	50

TABLE II. Sputtering conditions for deposition of Zn layers.

Sample	Power (W)	Thickness (nm)	Deposition time (s)	Substrate temperature (°C)
A	25	50	150	36
B	50	50	60	43
C	75	50	40	49
D[a]	75	50	40	49

[a]Samples of batch D were fabricated without the first Au layer.

The fabrication process was conducted as follows:

(1) Cleaning step: The samples were cut and then cleaned in an ultrasonic bath of acetone followed by an isopropanol ultrasonic bath and dried by N_2 blowing.
(2) Back contact deposition: A metallic multilayer Au/Zn/Au structure (20 nm/50 nm/250 nm) was deposited on the rough side of the substrate.
(3) Front contact deposition: Front round contacts, with the same metallic multilayer used in the back contact, were defined on the polished side of the samples by using a shadow mask.At this point, the I–V characteristics of the samples were measured. Results are shown in Fig. 2, where it is evident that the total resistance decreases as the RF sputtering power is increased. However, a clear rectifying behavior still remains in all the samples.An additional batch of samples (D) was fabricated without the first Au layer. The Zn layer was deposited at 75 W for this batch. The results were similar to those obtained for batch C. However, this experiment reveals that sputtering a Zn (50 nm)/Au (200 nm) structure does not present any adhesion problems.Finally, in order to extract the resistivity of the substrates, an additional step was required to form an ohmic contact on each sample using a conventional process. Figure 3(a) shows a top view of the samples described in this section. Front round contacts of five different sizes were defined.

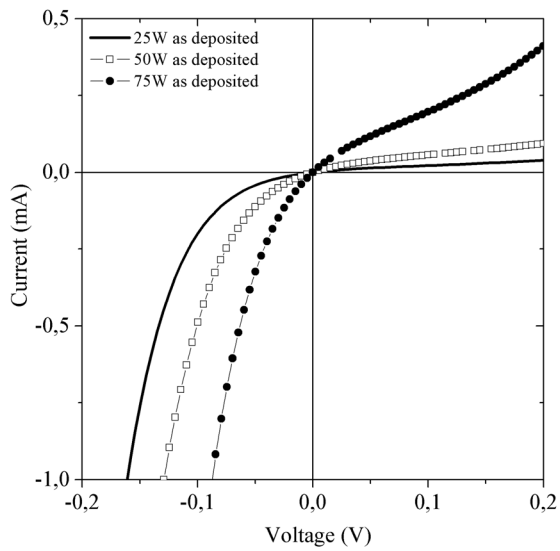

FIG. 2. I–V responses as a function of the Zn RF sputtering power.

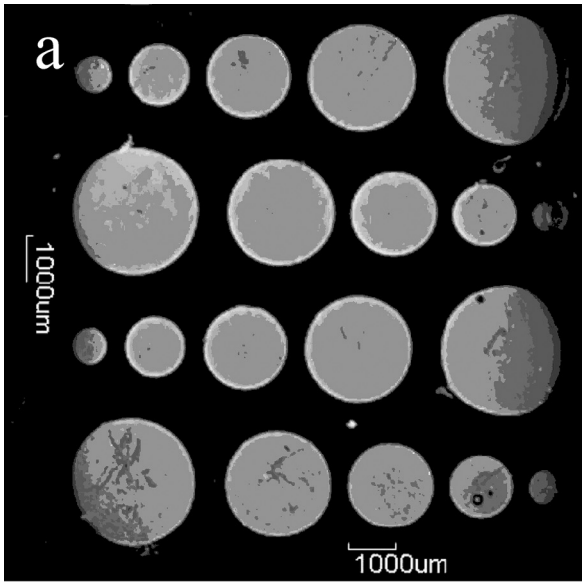

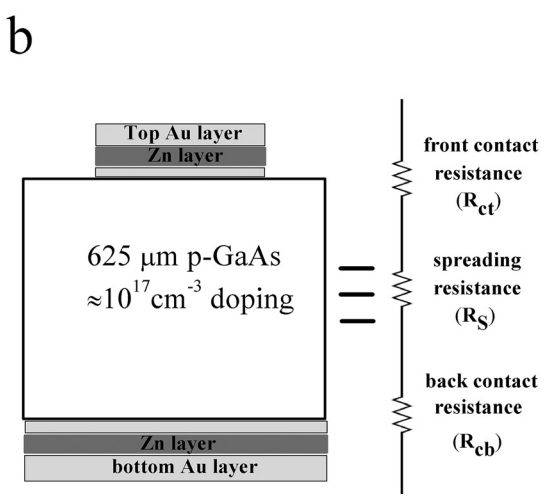

FIG. 3. (a) Top view of samples used in Sec. III A. (b) Equivalent resistance of the structure after RTA step.

(4) Rapid thermal annealing: This step was performed based on the conditions reported in a previous work.[4] Figure 3(b) shows the equivalent resistance of a structure after the RTA step. The total resistance can be calculated using the following equation:

$$R_T = R_S + R_{ct} + R_{cb}, \tag{1}$$

where R_S is the resistance corresponding to the bulk or spreading resistance, and R_{ct} and R_{cb} are the resistances of the front and back contacts, respectively. The round front contact area is completely defined, but the back contact area is unknown. Therefore, we decided to consider the worst case as $R_{cb} = R_{ct}$, when in fact $R_{cb} < R_{ct}$, which leads to

$$R_T \cong R_S + 2R_{ct}. \tag{2}$$

The expression below was chosen to calculate the spreading resistance, based on a previous analytical study[15]

$$R_S = \frac{\rho_b}{2\pi r}\arctan\left(\frac{2W}{r}\right), \tag{3}$$

where ρ_b is the substrate resistivity, r is the radius of the front round contact, and W is the distance between the front and the back contact, i.e., the thickness of the wafer.

By adjusting Eq. (2) with the curve obtained from the relation between the total resistance $R_T(r)$ and the front contact area, a substrate resistivity value of approximately $0.1 \pm 0.03\ \Omega$ cm was obtained. This fitting is only minimally affected by the approximation used in Eq. (2), because of the structure characteristics (radius r between 0.05 and 0.15 cm, thickness of 625 μm, and specific contact resistivity less than $10^{-4}\ \Omega\ \text{cm}^2$ reported in previous works for this contact).[4,5] Thus, the contact resistance term only represents approximately 3% of the total measured resistance.

B. Laser firing process study

In this section, the influence of laser-firing parameters on the electrical behavior of the metal–semiconductor contact and the morphology of the resulting crater (the disturbance to the contact topology produced by the laser heating) are analyzed. The fabrication process sequence varies from that detailed in Sec. III A. First, an ohmic contact was formed on the rough side of the sample using the conventional procedure of depositing the metallic multi-layer structure followed by a RTA step. Next, round front contacts with a radius of 1.25 mm were defined on the polished side by using a shadow mask [Fig. 4(a)]. Thus, the influence of the laser process was evaluated for an ohmic contact deposited on the back side of the sample and the as-deposited front side of the vertical structure. Figure 4(b) shows the equivalent electrical circuit of the structure before and after the laser-firing process.

The key parameters examined in the laser process were power (related to the energy of the beam), number of pulses (which can be interpreted as the duration of the thermal step), and pitch (distance between points of laser-firing contact).

1. Influence of the laser-firing power

The influence of the laser beam power was analyzed keeping the number of laser pulses (Np) fixed at 62 pulses. The laser power was varied in the range of 0.8–6.4 W. In our system, the minimum power that forms an ohmic contact is 1.7 W. The heating produced by the laser pulses at this power appears to be sufficient to drive Zn atoms into the GaAs substrate and create an ohmic contact.

Figures 5(a) and 5(b) show the effects of the laser power on total resistance and on radius of the resulting crater. As is visible in Fig. 5(b), the radius of the crater increases monotonically as the power increases. The inset shows the profile defining the typical crater. In contrast, the total resistance presents a minimum at 3.2 W of laser power. The crater area can be considered the contact area, so based on the relation between crater radius and laser power, we conclude that optimal laser power is in the range of 1.7–3.2 W.

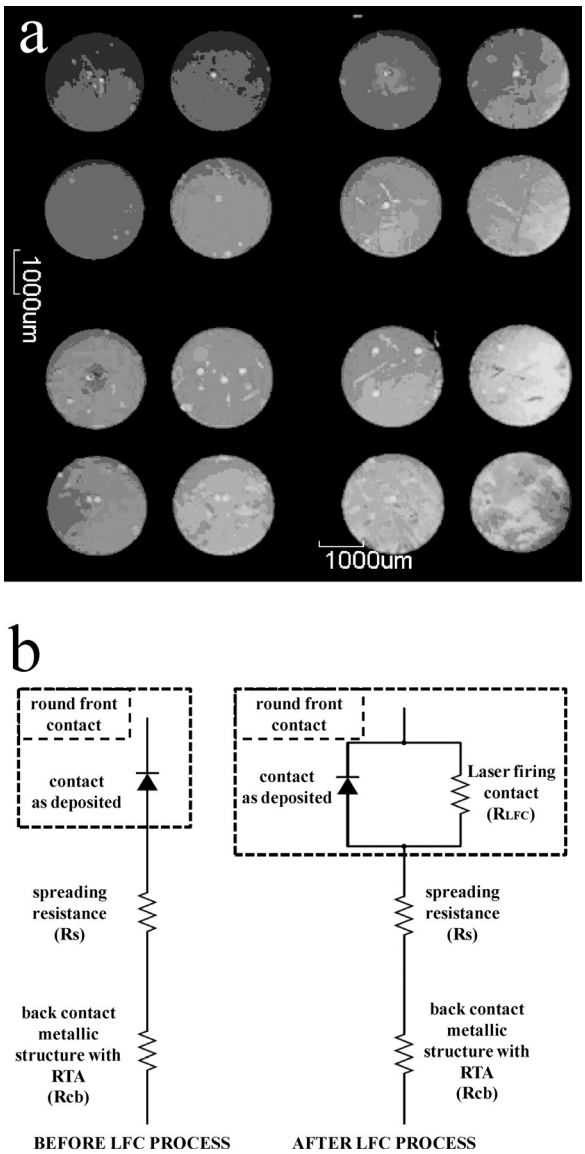

FIG. 4. (a) Top view of samples used in Sec. III B to carry out the laser process study. (b) Equivalent electrical circuit of samples used in Sec. III B, before and after laser-firing contact process on the front round contact.

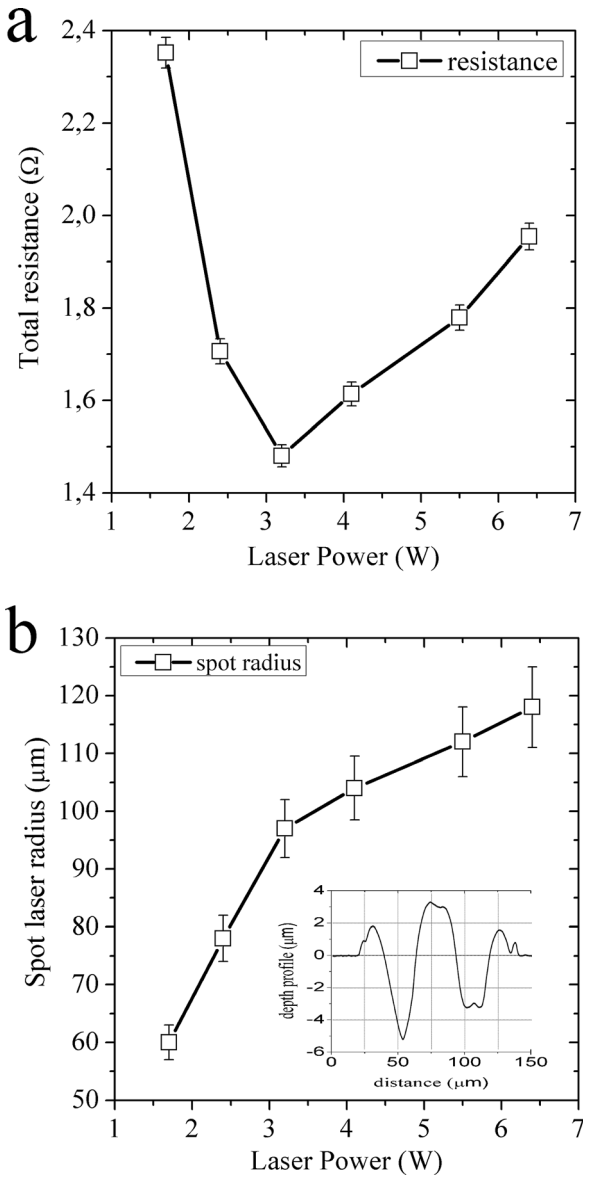

FIG. 5. (a) Effect of laser power on the total measured resistance. (b) Effect of laser power on the radius of the laser crater. The inset in the figure shows a depth profile of the crater created at 1.7 W.

In order to extract the specific contact resistivity, the worst case is again considered, supposing that all the contact resistance is due to the top laser-firing contact R_{LFC}, including R_{cb} in R_{LFC}. The measured resistance of the vertical structure follows the equation:

$$R_{measured} = R_S + R_{LFC}, \tag{4}$$

where R_S is the spreading resistance. The specific contact resistivity of the laser-firing contact can be evaluated as

$$R_{LFC} = \frac{\rho_{cef_{LFC}}}{\pi {r_{LFC}}^2}, \tag{5}$$

$$\rho_{cef_{LFC}} = \pi {r_{LFC}}^2 \left[R_{measured} - \frac{\rho_b}{2\pi r_{LFC}} \arctan\left(\frac{2W}{r_{LFC}}\right) \right]. \tag{6}$$

The theoretical value of the spreading resistance R_S, working with the substrate resistivity ρ_b extracted from Sec. III A and the radius r_{LFC} of the crater, is greater than the total resistance measured $R_{measured}$. This inconsistency is due to a contact area larger than the crater area considered, as will be shown in the following sections. Finally, a laser power of 1.7 W was selected to create shallow craters.

2. Influence of number of pulses

The Np parameter can be interpreted as the duration of the thermal process of the laser-firing. The value of Np has a great influence on the morphology of the spot crater as is evidenced by the SEM images shown in Figs. 6(a) and 6(b). Figure 6(a) shows a detailed view of the crater created by Np = 251 pulses, where a relatively smooth surface can be observed. Figure 6(b) shows a general view of the 158 μm diameter crater created using Np = 2000 pulses with a deep hole in the center.

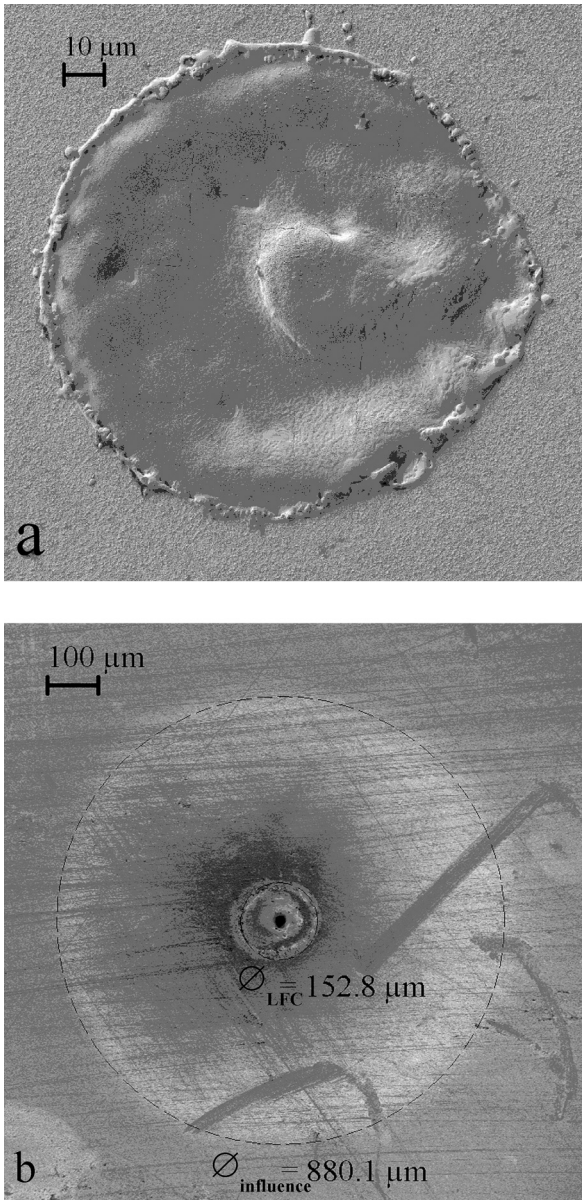

FIG. 6. SEM images: (a) detailed view of the crater using 1.7 W and 251 Np; (b) general view of the crater using 1.7 W and 2000 Np.

Increasing the Np value led to an increasing influence by the LFC area, which is manifested by a color change of the area near the crater, as observed with an optical microscope. This effect was also confirmed by SEM [Fig. 6(b)] where a clear topographic contrast in the area of about 880 μm of diameter surrounding the crater is mainly due to differences in the material, not topography changes. This circular area of laser influence around the crater is formed by local heating effects that cause an inter-diffusion between substrate and Au/Zn/Au deposited layers. The EDX analysis supports this conclusion.

The increase of Np also led to an increase in crater radius, as shown in Fig. 7. This effect is greater as the intensity increases, from a 5% increment of the crater radius at 1.7 W to 20% for 3.2 W. It was determined that a minimum of 62 pulses are needed to create the ohmic contact for a power of 1.7 W.

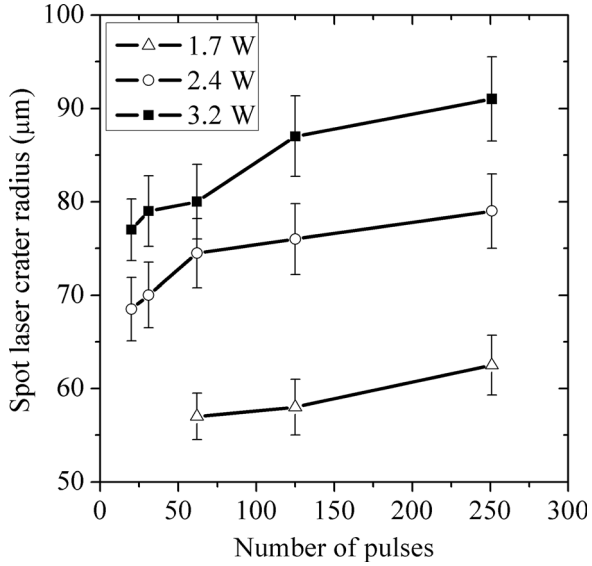

FIG. 7. Influence of the Np parameter on crater radius for three different powers.

Figure 8 shows the influence of Np on the total resistance. The ability to determine an exact specific contact resistivity value is restricted by the contact area evaluated. The SEM images presented in Fig. 6(b) show that the influence area can be five times greater than the crater, making it difficult to accurately determine the contact area. This fact explains the inconsistency discussed in Sec. III B 1.

3. Analysis of the laser-firing pitch effect

The pitch refers to the distance between two different LFC points. The role of the pitch depends on the kind of application. For example, in a previous work[11] studying ohmic contact formation by laser-firing process, the optimum pitch depends on the tradeoff between the total contact resistance and the deterioration of the passivation. In this work, the study of pitch is related to the premise that the

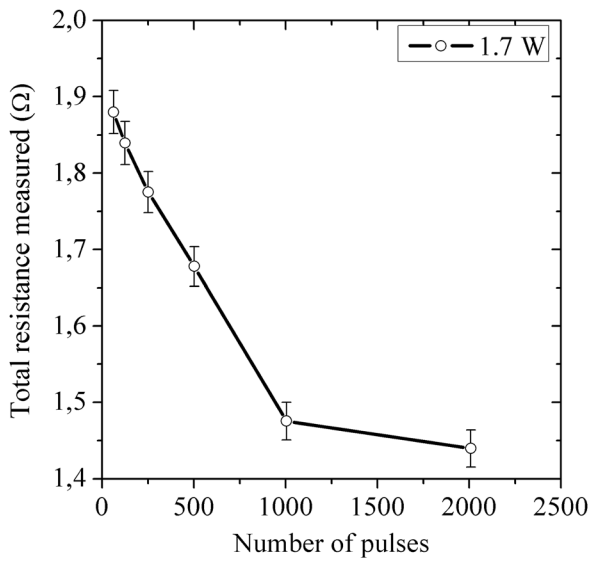

FIG. 8. Total resistance measured as a function of the Np parameter for 1.7 W.

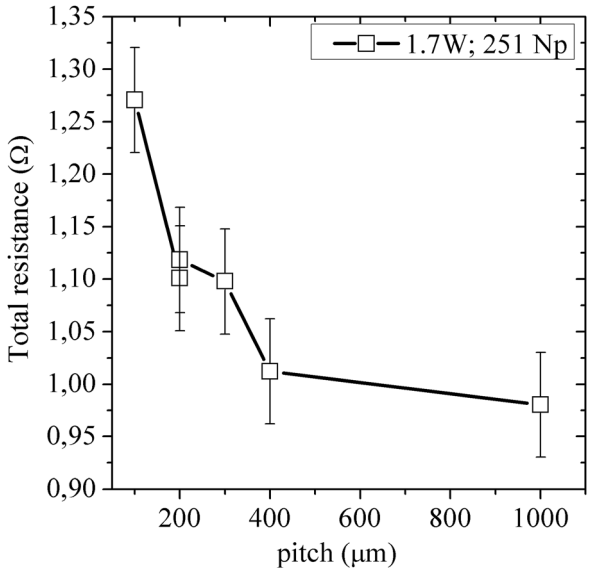

FIG. 9. Influence of the pitch parameter on the total resistance measured for 1.7 W and 251 Np.

influence area of the LFC point is larger than the morphological evidence represented by the crater, as discussed in previous sections.

The pitch study was carried out using two LFC points on the same front round contact. In theory, two LFC points should act like two parallel resistances, so the total resistance should be half. This is true as long as the LFC areas do not overlap. Figure 9 shows how the pitch influences the total resistance measured for 1.7 W and Np = 251 pulses. The total resistance decreases as the pitch increases. This trend indicates that as the distance between two LFC points is increased, the area of LFC overlap is reduced. From Fig. 9, it can be concluded that pitch values greater than 400 μm do not imply an effective reduction of the total resistance measured. Therefore, it can be concluded that the radius of the effective contact area is $200 \pm 10\,\mu$m, which is 3.2 greater than the radius of the measured crater (Fig. 7) for 1.7 W and Np = 251 pulses. If Eq. (6) is applied using this effective contact area and the $R_{measured}$ shown in Fig. 8, then the value obtained for the $\rho_{cef_{LFC}}$ is $1.5*10^{-4}\ \Omega\ cm^2$ for 1.7 W and Np = 251 pulses. The LFC area depends on both the laser power and the Np value. The LFC area depends on both the laser power and the Np value.

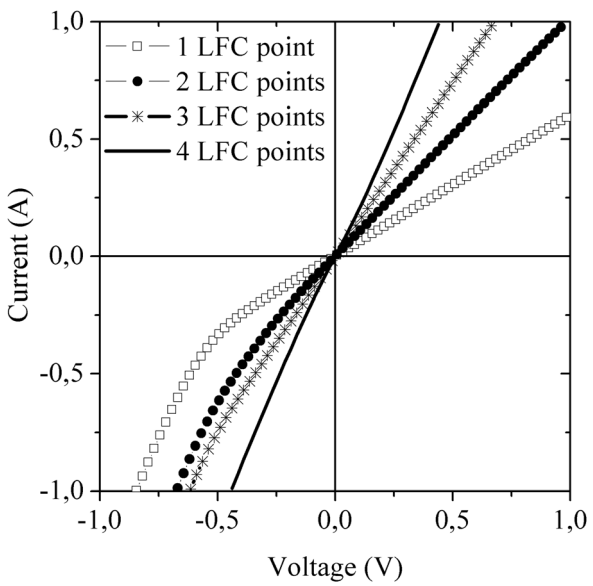

FIG. 10. I–V responses depending on the number of LFC points on the same front round contact using 1.7 W and 251 Np.

The final experiment consisted of increasing the number of LFC points on the same top contact with a pitch of 600 μm. Figure 10 shows the change in the structures I–V characteristics when the number of LFC points increases. This result verifies the equivalent electric circuit proposed in Fig. 4(b). Although this study reinforces the difficulty in determining the contact area, it demonstrates that using four LFC points causes the total resistance measured to be less than double the contact resistance of a 1.25 mm radius pad formed using the conventional process with a RTA step, which means a specific contact resistivity less than $2*10^{-4}\ \Omega\ cm^2$.

IV. CONCLUSIONS

A novel approach is used to form ohmic contacts on moderately p-doped GaAs substrates. The process avoids thermal stress to the whole structure associated with typical annealing steps. The ohmic contacts are fabricated by sputtering an Au/Zn/Au structure and using a laser-firing technique.

The influence of the RF sputtering power on Zn layer deposition was analyzed. Results do not show a relevant impact of this parameter on the rectifier behavior of the metal–semiconductor contact.

In laser-firing study, we explored the influence of different parameters on the electrical response and morphology of the resulting crater. A minimum laser power of 1.7 W is necessary in our system to produce Zn diffusion into the GaAs and create the tunneling contact. A study of the influence of Np (number of pulses) revealed that the area of influence is larger than the crater. This effect is substantiated by SEM images and EDX analysis.

A study of pitch led us to conclude that the radius of the effective contact area can be 3.2 greater than the crater radius. This study shows that using four LFC points on the same front round contact allowed us to achieve a specific contact resistivity less than $2*10^{-4}\ \Omega\ cm^2$.

ACKNOWLEDGMENTS

This work was partially supported by The Spanish Ministry of Education and Science under the Consolider Ingenio 2010 Program, through the project GENESIS-FV (CSD2006-0004). Thanks to Trifon Trifonov for the SEM images and EDX analysis.

[1]V. L. Rideout, Solid State Electron. **18**, 541 (1975).
[2]T. C. Shen, G. B. Gao, and H. Morkoç, J. Vac. Sci. Technol. B **10**, 2113 (1992).
[3]A. G. Baca, F. Ren, J. C. Zolper, R. D. Briggs, and S. J. Pearton, Thin Solid Films **308–309**, 599 (1997).

[4]Yicheng Lu, T. S. Kalkur, and C. A. Paz de Araujo, J. Electrochem. Soc. **136**, 3123 (1989).
[5]T. Sanada and O. Wada, Jpn. J. Appl. Phys. **19**, L491 (1980).
[6]F. Ren, C. R. Abernathy, S. J. Pearton, and J. R. Lothian, J. Vac. Sci. Technol. B **13**, 293 (1995).
[7]H. Cotal, C. Fetzer, J. Boisvert, G. Kinsey, R. King, P. Hebert, H. Yoon, and N. Karam, Energy Environ. Sci. **2**, 174 (2009).
[8]G. J. Bauhuis, P. Mulder, E. J. Haverkamp, J. C. C. M. Huijben, and J. J. Schermer. Sol. Energy Mater. Sol. C **93**, 1488 (2009).
[9]P. G. Linares *et al*., Sol. Energy Mater. Sol. C **108**, 175 (2013).
[10]O. Moutanabbir and U. Gösele, Annu. Rev. Mater. Res. **40**, 469 (2010).
[11]P. Ortega, A. Orpella, I. Martín, M. Colina, G. López, C. Voz, M. I. Sánchez, C. Molpeceres, and R. Alcubilla, Prog. Photovolt: Res. Appl. **20**, 173 (2012).
[12]W. Brendle, V. X. Nguyen, A. Grohe, E. Schneiderlöchner, U. Rau, G. Palfinger, and J. H. Werner, Prog. Photovolt: Res. Appl. **14**, 653 (2006).
[13]I. Sánchez-Aniorte, R. Barrio, A. Casado, M. Morales, J. Cárabe, J. J. Gandía, and C. Molpeceres, Appl. Surf. Sci. **258**, 9443 (2012).
[14]K. Wasa and S. Kayakawa, *Handbook of Sputter Deposition Technology* (Noyes Publications, NJ, 1992), 64 pp.
[15]M. W. Denhoff, J. Phys D: Appl. Phys. **39**, 1761 (2006).